MINERALOGICAL MAGAZINE

VOLUME 56 NUMBER 382 MARCH 1992

1966 ash eruption of the carbonatite volcano Oldoinyo Lengai: mineralogy of lapilli and mixing of silicate and carbonate magmas

J. B. DAWSON

Department of Geology and Geophysics, University of Edinburgh, West Mains Road, Edinburgh EH9 3JW

AND

J. V. SMITH AND I. M. STEELE

Department of the Geophysical Sciences, University of Chicago, Illinos 60637, U.S.A.

Abstract

Lapilli from the August 1966 eruption of the carbonatite volcano Oldoinyo Lengai consist of carbonate-cemented aggregates of (i) mono- and poly-mineralic fragments of ijolitic rocks, (ii) single grains and clusters of euhedral nepheline, Ti-andradite, and Ti-magnetite, and (iii) corroded pyroxene and wollastonite grains surrounded by coronas containing combeite, melilite, Ca-silicates (possibly larnite and rankinite), and rounded bodies of submicrometre intergrowths with complex bulk compositions dominated by Na,K,Ca-phosphate-carbonate and alkali-iron-sulphide-carbonate. The (ii,iii) materials, together with abundant Na-carbonate, sylvite and fluorite occurring as cement and shells in the lapilli, are attributed to mixing and incomplete reaction of ijolite and carbonatite magmas during the explosive eruption. The rounded submicrometre intergrowths are interpreted as the quench products of two types of immiscible liquids whose properties should be studied by controlled synthesis.

KEYWORDS: carbonatite, silicate, carbonate, magmas, Oldoinyo Lengai, ash.

Introduction

THE extrusion of the alkali carbonatite lavas at Oldoinyo Lengai (Dawson, 1962*a*,*b*), first observed in 1960, has attracted considerable attention. As a result, the petrology, chemistry and physical properties of these unusual lavas are now well documented (Dawson, 1989; Dawson *et al.*, 1990; Keller and Kraft, 1990; Peterson, 1990). Lava was extruded from 1960 to late July 1966 and again from April 1983 to at least January 1991.

Ash eruptions occurred from mid-August to early October 1966, in July 1967, and in January 1983. The violent explosion in August 1966 ended the six-year period of quiet extrusion of lava. A description of this eruption (Dawson *et al.*, 1968) reported 25% SiO_2 in the ash, in contrast with the nil-silicate lavas. The ash contains melanite garnet, pyroxene, Na-melilite, nepheline, Ti-magnetite and wollastonite crystals, as well as traces of combeite, larnite, rankinite, natrite, sylvite, baryte and Na,Ca, K-phosphate minerals. In an abstract, Smith *et al.* (1988) also reported K,Na,Fe,Mn,Si,P,Cl-sulphide and carbonate differentiates and complex reaction textures.

Mineralogical Magazine, March 1992, Vol. 56, pp. 1–16

Dawson *et al* (1989) described the compositional range of the combeite, near $Na_{2.3}Ca_{1.7}Si_3O_9$, and its occurrence both as euhedra and as a component of coronas around Ca-bearing silicates in contact with sodium carbonatite magma.

We supplement these reports with a detailed description of the petrography and mineralogy, and discuss the evidence for complex liquids containing carbonate, sulphide, silicate, alkalis, halogens and phosphorus components.

Petrography

Lapilli in sample BD882, collected from the eastern rim of the crater on August 21, 1966, are up to 2 mm across. They were stored in a sealed plastic bag to inhibit hydration of the alkali carbonate.

The lapilli consist of large grains (0.5–1 mm) or aggregates of grains together with a 'cloud' of smaller grains (often <20 μm), all cemented by carbonate into spheroidal nodules (Fig. 1). Rare nodules lack the large grains. Individual lapilli may consist of a single nodule, or a central nodule surrounded by several concentric shells of carbonate-cemented dust, separated by carbonate. The small grains are euhedra of nepheline, combeite, Ti-andradite garnet, melilite and Ti-magneitite. Numerous micrometre to submicrometre grains of sylvite were found in the carbonate matrix using back-scattered electron imaging and potassium and chlorine X-ray imaging. They had not been recognized in the original optical study, but were found when a search was made for the K- and Cl-bearing minerals necessary to account for these elements in the bulk analysis. Sylvite also occurs in the carbonatite lavas (Dawson, 1989). A search for the host of fluorine revealed scattered X-ray peaks for F in a scanning image of the carbonate matrix. Since fluorite occurs in the Lengai carbonatite lavas, these F concentrations in the ash are attributed to tiny crystals of this mineral. Unfortunately the association of Ca with F could not be tested with certainty because Ca from supposed fluorite microcrystals would be swamped by the Ca signal from other more abundant minerals. There are also rare 5–10 μm spherules of a complex silicophosphate. Baryte and Fe-alabandite occur as small grains in the carbonatite lavas (Keller and Krafft, 1990; Peterson, 1990).

The larger grains and grain aggregates are of two types:

(i) Single crystals, and aggregates of various combinations of anhedral grains, of nepheline, clinopyroxene, wollastonite and Ti-andradite. The aggregates are interpreted as fragments of ijolites (Fig. 1A), such as those present in the stratigraphic volcanic pile and those ejected during the 1966 eruption. They have similar grain size and chemical composition. The single crystals have similar chemical compositions, and commonly have fractured margins, and are attributed to fragmentation of solid ijolites.

(ii) Euhedral single grains of nepheline, garnet and combeite (Fig. 1B). Nepheline has concentric inclusions of apatite and pyroxene, and combeite has inclusions of nepheline, melilite, garnet and Ti-magnetite. Acid-leached concentrates yielded aggregates of euhedra of nepheline + nepheline, garnet + garnet, and nepheline + garnet (Figs. 2, 3). One example of euhedral nepheline + euhedral garnet + anhedral pyr-

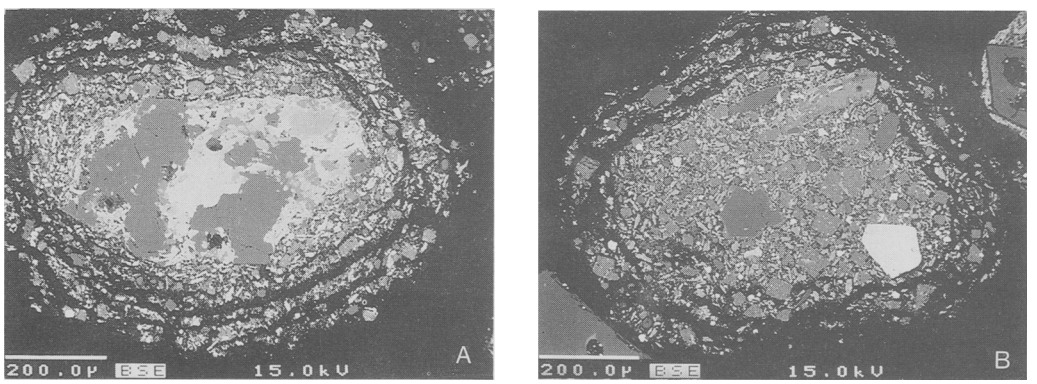

FIG. 1. BSE images of lapilli showing cores surrounded by concentric shells. A has a core of ijolite with anhedral grains of nepheline (light grey), pyroxene (medium grey) and garnet (white). B has euhedra of nepheline (medium grey), garnet (white), and combeite (medium grey, speckled). Both lapilli contain a host of microphenocrysts cemented by alkali carbonate (black). The concentric shells are separated by alkali carbonate.

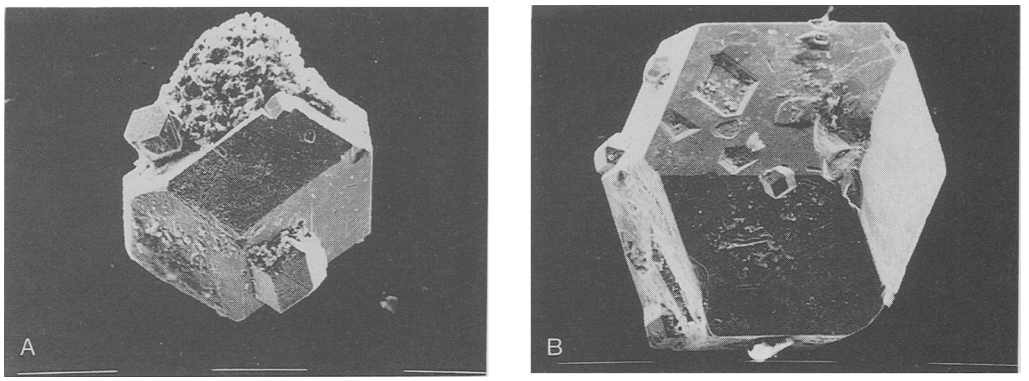

FIG. 2. Scanning electron micrographs of euhedra. (A) An aggregate of two garnet crystals (dodecahedra), a hexagonal prism of nepheline, and the corroded relic of a pyroxene. B is a large garnet crystal with five smaller garnets attached to the surface and several depressions with crystal faces that would correspond to loss of attached crystals. Scale bar is 100 μm.

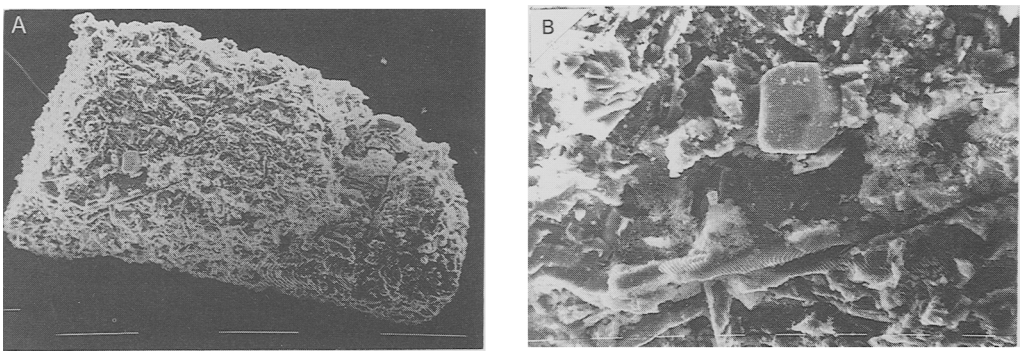

FIG. 3. Scanning electron micrographs of a corroded pyroxene crystal (A) with a coating of melilite laths, scale bar is 100 μm. B is an enlargement of middle left of 3A showing an attached garnet that survived corrosion; scale bar is 10 μm.

oxene was found (Fig. 2A): tiny melilite grains coated the pyroxene as in the combeite-melilite coronas around single pyroxene grains. Apart from this pyroxene, all grains showed excellent crystal faces, particularly the garnets that show delicate growth features (Fig. 2B). They have similar morphology to the smaller dust grains, in contrast to the anhedral, fractured grains attributed to breakup of an ijolite parent. Hence the euhedral grains were growing in the magma associated with the 1966 eruption.

Fragments of alkali carbonatite lava show trachytic textures of aligned nyerereite and gregoryite phenocrysts, similar to the lavas extruded on the crater floor before the 1966 eruption.

Most lapilli are cemented by, and may have one or more concentric shells of, alkali carbonate which scatters electrons weakly. Previously, we have described pyroxene and wollastonite grains with combeite and melilite coronas which were interpreted as the reaction products with an alkali carbonate (Dawson, *et al.*, 1989). Because of the corrosion of the outer boundary, the petrogenetic position of the pyroxene crystals is uncertain when they are not attached to a euhedral crystal as in Fig. 2A, Fig. 3 is a SEM photograph of a leached pyroxene crystal with an overgrowth of melilite laths: the combeite overgrowths were leached by weak HCl solution. Fig. 4 shows an unfractured pyroxene crystal with delicate oscillatory zoning right up to the corroded margin, and is probably the relic of a phenocryst. Whether any of the corroded pyroxene crystals derive from fragmented ijolite blocks is uncertain. Within the replacement coronas (Fig. 5) there are small rounded to amoeboid inclusions (up to 10 μm) of a K-bearing sulphide-rich phase (Fig. 6). Rare 10 μm grains of Ca-silicates, perhaps larnite and

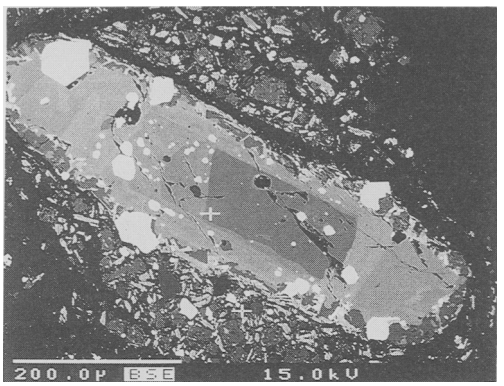

FIG. 4. BSE image of elongated, zoned pyroxene crystal in lapillus 6. Oscillatory zoning up to the grain margin indicates that the crystal might be a corroded phenocryst. Absence of fractures argues against violent disruption of an ijolite rock. Bright inclusions are Ti-garnet and Ti-magnetite.

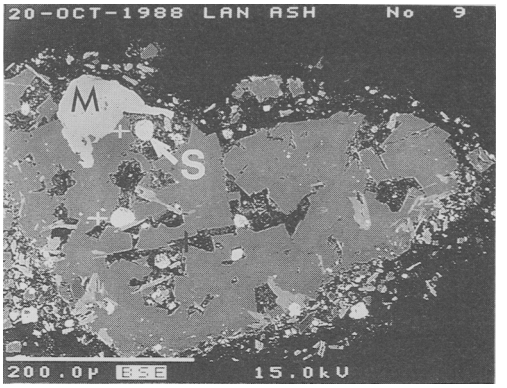

FIG. 6. BSE image of combeite crystal (medium grey) containing melilite laths (light grey). A magnetite crystal (M) with irregular outlines is partly enclosed by combeite. Alkali carbonate (black) occupies the interstices between the combeite crystals, and is a matrix for the microphenocrysts in the corona. Two rounded bodies of sulphur-rich alkaline material lie near the white crosses, and several others occur elsewhere; that labelled S is shown at greater magnification in Fig. 7.

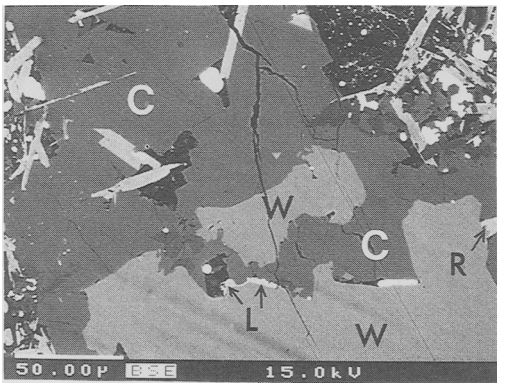

FIG. 5. BSE image of part of a wollastonite crystal (light grey, W) surrounded by a reaction rim of combeite (dark grey, C) and melilite blades (light grey). The S-rich phase is represented by the rounded to amoeboid white areas. Larnite (L) and rankinite (R) occur at the boundary between wollastonite and combeite.

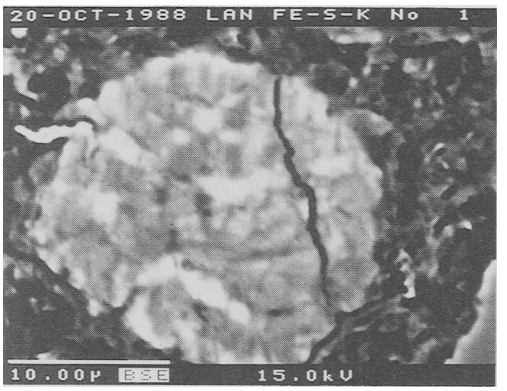

FIG. 7. BSE image of a sulphur-rich alkaline material. Shown at lower magnification in Fig. 6 (labelled S).

rankinite, occur at the interface between wollastonite and replacing combeite (Fig. 5). In BSE images, one of the sulphide-rich phases is mottled at the micrometre scale (Fig. 7) and must consist of at least two and possibly four chemical phases, at least one of which is sulphur-rich. The other sulphide-rich phases are optically homogeneous at the limit of optical resolution.

Mineral chemistry

Polished sections were prepared using diamond powder suspended in Vaseline, coated with a carbon film, and stored in a dessicator. Back-scatttered electron (BSE) images and electron microprobe analyses (15 keV, PAP correction program) were obtained on a Cameca SX-50 instrument. Almost all analyses were made in duplicate with movement of the electron beam to an adjacent spot to check for accidental overlap onto any sub-micrometre inclusion not visible in the BSE image. All deviations greater than 3

Table 1 Representative pyroxene analyses

	1	2	3	4	5	6	7	8	9	10
SiO_2	52.29	53.06	51.87	51.71	47.84	49.46	50.77	50.83	51.23	50.29
TiO_2	1.04	0.81	0.72	0.48	2.64	1.94	0.64	0.35	0.26	0.48
Al_2O_3	1.04	0.82	0.98	0.58	3.13	1.56	0.43	0.60	0.57	0.55
Cr_2O_3	0.00	0.00	0.01	0.01	0.00	0.00	0.00	0.00	0.00	0.00
FeO	7.18	7.04	12.08	16.71	13.30	6.31	12.82	19.14	15.99	20.24
MnO	0.26	0.19	0.35	0.57	0.43	0.46	0.84	0.91	1.01	1.07
MgO	13.90	14.80	10.61	7.92	9.31	15.12	10.72	5.67	7.95	4.81
NiO	0.00	0.01	0.02	0.03	0.08	n.a	n.a	n.a	n.a	n.a
CaO	24.55	24.19	22.48	19.79	22.10	24.49	21.76	18.39	20.37	17.19
Na_2O	0.82	0.96	1.81	3.12	1.75	0.71	1.48	2.95	1.75	3.38
K_2O	0.01	0.01	0.00	0.00	0.09	0.01	0.02	0.00	0.00	0.00
Sum	101.09	101.89	100.93	100.92	100.67	100.06	99.48	98.84	99.13	98.01

1-3: Core (1) and opposite ends (2,3) of grain 1.
4: Grain 12 with two attached garnets (see table 2).
5: Inclusion in nepheline 16 (see table 3).
6-10: Core (6) intermediate zones (7,8,9) and rim (10) in zoned grain in lapillus 6 (see fig. 4).

Analyses 1-5 were made on grains in acid leaches.

sigma statistical fluctuation were checked by further analysis. The beam current and spot size were adjusted so that no specimen damage occurred even for the unstable materials. For submicrometre intergrowths it was not possible to obtain accurate analysis of the individual phases but semiquantitative correlations were obtained for the major elements using the scanning mode. The X-ray signal from carbon was detected using a lead stearate monochromator. Qualitative analyses were obtained using dolomite as a standard. However quantification was not possible, especially for low concentrations, because of the difficulty in determining the background and the matrix correction factors. Il general, caution is needed with respect to a minmr or trace element in analyses of all the small grains because of the problem of secondary fluoresence from neighbouring grains with a high concentration of the element. Another problem for light elements is that the correction program assumes that the unanalysed component is all oxygen whereas carbon and fluorine are present in some materials. Scanning electron images were made on individual grains released by dilute HCl.

Pyroxene. Chemical variation occurs between and within grains (Table 1). Generally, the pyroxenes have low alumina and negligible chromium and nickel. Variations are mainly in the diopside/hedenbergite ratio, and less so in the aegirine component. Overall, the compositions fall within the ranges for the pyroxenes in the silicate lavas at Oldoinyl Lengai (Donaldson *et al.*, 1987) and in the plutonic ijolite and nepheline syenite blocks in the pyroclastic rocks (unpublished). The present grains do not have an Fe-rich rim like those in the lavas and plutonic blocks, perhaps because there was no trapped Fe-rich liquid. Marginal replacement of the pyroxenes of the ash by combeite-melilite coronas might have removed any Fe-rich rims that did form.

Garnet. All garnets (Table 2) are andradite with low alumina and magnesia (less than 1

Table 2. Representative analyses of garnets in acid leaches

	1	2	3	4	5	6	7
SiO_2	30.23	28.07	30.07	31.91	29.71	30.06	31.18
TiO_2	13.59	17.00	13.87	10.41	14.68	15.82	10.77
Al_2O_3	0.61	1.03	0.53	0.89	0.42	0.72	0.98
Cr_2O_3	0.00	0.00	0.00	0.06	0.00	0.02	0.02
FeO	21.16	19.52	21.13	22.60	21.17	19.38	21.78
MnO	0.41	0.37	0.42	0.38	0.37	0.31	0.35
MgO	0.37	0.34	0.80	0.37	0.45	0.34	0.37
NiO	0.02	0.00	0.00	0.00	0.04	0.09	0.10
CaO	32.58	32.75	33.40	33.40	32.42	33.20	33.01
Na_2O	0.51	0.39	0.42	0.36	0.66	0.45	0.38
K_2O	0.01	0.00	0.00	0.01	0.00	0.00	0.02
Sum	99.49	99.47	100.64	100.39	99.92	100.39	98.96

1: Average of core and rim of near-homogeneous grain attached to pyroxene.
2-3: Core (2) and rim (3) of inhomogeneous grain.
4: Grain 12A, enclosing nepheline.
5: Grain 12, attached to pyroxene (see Table 1)
6: Small grain.
7: Attached to nepheline grain 16 (see Table 3).

wt.%), and negligible Cr_2O_3 and NiO (<0.1%). Titania varies the most (10.4–17.0 wt.%), with an inverse correlation with Fe. Silica and lime vary little. The garnets contain small, but significant, amounts of Na_2O (0.31–0.66 wt.%). Sodium is normally negligible in garnets from the earth's surface, while small amounts occur in garnets formed at high pressure in eclogites and peridotites from the upper mantle. Coupled substitutions such as $Ca^{viii} + Si^{iv} = Na^{viii} + P^{iv}$ and $Ca^{viii} + Al^{vi} = Na^{viii} + Ti^{vi}$ are believed to be responsible for the sodium substitution at high pressure (Bishop *et al.*, 1978). However, the Oldoinyo Lengai garnets did not grow at high pressure, and their Na content is probably due to crystallization from peralkaline magma. Overall, the compositions fall within the ranges for the garnets from the lavas and plutonic blocks.

Wollastonite. Apart from CaO and SiO_2, the only oxides of significance are Fe_2O_3 ($\approx$ 1 wt.%) and MnO (0.43 wt.%) The average composition (Table 3) falls within the compositional range for wollastonite in other Oldoinyo Lengai rocks.

Nepheline. The composition is variable from grain to grain, and between cores and rims (Table 3). One grain has higher CaO (0.66 wt.%) and lower Fe_2O_3 (0.96 wt.%) than the other grains which have about 2 wt.% Fe_2O_3. Another grain has a rim more potassic (Ks_{24}) than the normal range (Ks_{17-20}). Overall the compositions match those in the other lavas and plutonic blocks from Oldoinyo Lengai. However, no analysed grain reaches the high Fe_2O_3 (5 wt.%) of a nepheline enclosed by a combeite phenocryst (Dawson *et al.*, 1989).

Combeite. The analyses in Table 3 are representative of the larger number given by Dawson *et al.* (1989). The average formula $Na_{2.33}Ca_{1.74}$ others$_{0.12}Si_3O_9$ departs from ideal $Na_2Ca_2Si_3O_9$ because of solid solution towards the $Na_6Si_3O_9$ component. There are no significant differences in composition between the combeite replacing wollastonite and pyroxene grains, and the combeite phenocrysts and microphenocrysts.

Magnetite. The main substituent apart from the iron oxides is TiO_2 which is variable from grain to

TABLE 3. Analyses of other phases in acid leaches

	1	2	3	4	5	6	7	8	9	10	11	12
SiO_2	51.06	30.04	41.67	41.17	43.38	41.21	42.34	50.02	50.50	0.51	0.25	0.14
TiO_2	0.06	38.70	0.02	0.01	0.04	0.01	0.01	0.16	0.21	0.03	8.72	3.16
Al_2O_3	0.02	0.39	35.04	33.93	33.28	34.22	32.16	0.00	0.06	0.00	0.11	0.13
Cr_2O_3	0.00	0.01	0.00	0.00	0.00	0.00	0.00	0.02	0.01	0.00	0.02	0.01
Fe_2O_3	1.07	1.80	0.95	1.96	2.17	1.93	2.79	0.29	0.44	0.02		
FeO	-	-	-	-	-	-					81.64	84.24
MnO	0.43	0.01	0.00	0.00	0.01	0.00	0.01	0.28	0.32	0.00	1.55	2.00
MgO	0.17	0.00	0.03	0.02	0.03	0.01	0.02	0.07	0.24	0.00	0.58	0.46
NiO	0.00	0.00	0.00	0.00	0.00	0.00	0.00	0.04	0.12	0.00	0.04	0.00
CaO	47.81	28.54	0.66	0.14	0.15	0.10	0.11	28.16	27.15	57.3	0.36	0.04
Na_2O	0.03	0.15	17.22	15.92	17.20	17.40	16.26	20.56	20.66	0.13	0.05	0.03
K_2O	0.00	0.02	5.86	7.96	5.61	6.45	7.28	0.19	0.23	0.01	0.00	0.00
Sum	100.48	99.65	101.45	101.11	101.87	101.33	100.95	99.79	99.94	-		

1.Wollastonite: mean of 9 analyses of three unzoned grains that are isochemical within analytical error. 2.Titanite; mean of two analyses of one grain. 3. Nepheline: Ca-rich, Fe-poor grain 16 with pyroxene inclusion (see Table 1). 4.Nepheline: K-rich-rim of nearly-homogeneous grain. 5.Nepheline: K-poor grain enclosed in garnet 12 (see Table 2). 6.Nepheline: near-homogeneous grain, with intermediate K; mean of 4 analyses. 7.Nepheline: Fe-rich rim of zoned, generally-Fe-rich grain. 8,9.Combeite. 10. Apatite: mean of two analyses of one grain; P not analysed. 11.Magnetite: mean of two analyses of nearly-homogeneous grain (TiO_2 8.59, 8.85). 12.Magnetite: mean of two analyses of nearly-homogeneous grain (TiO_2 3.19, 3.12).

Table 4 Analyses of melilites

	1	2	3	4
P_2O_5	0.27	0.07	0.10	0.01
SiO_2	42.41	42.70	42.77	43.64
TiO_2	0.28	0.07	0.02	0.10
Al_2O_3	0	4.19	5.11	4.31
FeO	9.33	6.69	10.14	8.42
MnO	1.99	0.61	0.37	0.41
MgO	7.58	7.04	4.36	3.16
CaO	35.81	33.92	30.75	29.46
SrO	n.a.	2.20	0.86	1.02
Na_2O	1.34	3.63	5.25	8.19
K_2O	0.22	0.29	0.35	0.34
SO_3	n.a.	0.06	0.01	0.02
Cl	n.a.	0.01	0.01	0.05
Sum	99.23	101.48	100.10	99.13

1. In corona replacing wollastonite, in lapillus 16.
2. In corona replacing wollastonite in lapillus 16.
3. Microphenocryst in dust, lapillus 15.
4. Inclusion in combeite, lapillus 15.

grain: e.g. 3.2 and 8.7 wt.% (Table 3). Spinel (*sensu stricto*) solid solution is insignificant.

Melilite. Analyses of melilite in the combeite/melilite reaction rims around pyroxene and wollastonite are given in Dawson *et al.* (1989). Melilite is variable in composition, both within individual coronas and between coronas, but the ranges overlap for coronas around pyroxene and wollastonite. All melilites contain substantial Na_2O (1.3–8.2 wt.%) and SrO (0.9–2.2 wt.%). Those occurring as microphenocrysts and inclusions in combeite tend to be more sodic and have lower SrO content (Table 4).

Calcium silicates. Two calcium silicates occur as 10 μm grains at the interface between residual wollastonite and replacing combeite (Fig. 5). These phases will be tentatively identified as larnite and rankinite on the basis of the chemical composition (Table 5) and paragenesis; however, diffraction data are needed for a positive identification. The possibility that these are new minerals with distinctive crystal structures should not be ruled out.

The 'larnite' (Table 5, anal. 3) yielded an analysis dominated by Ca and Si with only minor amounts of Na, Sr, K, Si and Mn. The atomic ratio $(R^{2+} + R^{1+})/(Si + P)$ of 2.13/0.94 deviates somewhat from the ideal value of 2 for calcium disilicate which has several polymorphs (Smith *et al.*, 1961). Perhaps a minor amount of $CaCO_3$ may be substituting for Ca_2SiO_4. Recent papers

Table 5 Analyses and structural formulae of Ca-silicates

	1	2	3	4	5		1	2	4
P_2O_5	0.01	0	-	0.25	-	P	0	0	.006
SiO_2	41.69	42.31	41.7	31.66	34.9	Si	2.006	2.022	.932
TiO_2	0	0	-	0.01	-	Ti	0	0	0
Al_2O_3	0.33	0.39	-	0	-	Al	.019	.022	0
FeO	8.00	7.95	-	0	-	Fe	.322	.318	0
MnO	0.85	0.90	-	0.16	-	Mn	.035	.036	.004
MgO	8.56	8.64	-	0.06	-	Mg	.614	.616	.004
CaO	35.83	35.45	58.3	65.82	65.1	Ca	1.847	1.815	2.066
SrO	1.58	1.47	-	0.34	-	Sr	.045	.041	.005
Na_2O	1.70	1.76	-	0.72	-	Na	.158	.164	.040
K_2O	0.19	0.12	-	0.36	-	K	.010	.007	.007
Cl	0.11	0.08	-	0.06	-				
S	0.02	0.04	-	0.02	-	Sum	5.056	5.041	3.064
						0	7	7	4
Sum	98.87	99.11	100.0	99.46	100.0				

1,2 "Rankinite", contact between combeite and wollastonite, lapillus 3
3 $Ca_3Si_2O_7$
4 "Larnite", contact between combeite and wollastonite, lapillus 3 (see fig 5)
5 Ca_2SiO_4

on the natural occurrence and phase equilibria of larnite (Saalfeld, 1975; Sabine, 1975; Sarkar and Jeffery, 1978; Shmulovich, 1968; Zharikov and Shmulovich, 1969) provide information that is not inconsistent with larnite forming in the Oldoinyo Lengai ash from Ca and Si released from wollastonite by the invading CO_2,. The trivial amount of Mg in the Oldoinyo Lengai specimen rules out bredigite.

The 'rankinite' (Table 5, anals. 1 and 2) contains substantial amounts of MgO (8.6 wt.%), FeO (8.0), Na_2O (1.7), SrO (1.55) and MnO (0.9). The ratio $(R^{2+} + R^{1+})$/Si is very close to 1.5. Both rankinite (Agrell, 1965; Henmi *et al.*, 1975; Kusachi *et al.*, 1975; Saburi *et al.*, 1976) and kilchoanite (Agrell and Gay, 1961; Mitsuda and Fukuo, 1969; Taylor, 1971) have this atomic ratio, and the former is tentatively preferred simply because kilchoanite appears to be a retrograde product of rankinite in nature, and there is no evidence for hydroxyl in Lengai volcanic rocks. However, all natural specimens of rankinite and kilchoanite are almost pure calcium silicates, and the substantial amounts of substituents in the Oldoinyo Lengai material might result in quite different phase equilibria and perhaps even a different structure type.

Whatever the exact mineralogical identification of the Oldoinyo Lengai materials, there is no doubt about the difference in paragenesis with respect to the occurrence of rankinite and larnite in marbles or limestones containing flint or chert that have undergone extreme thermal metamorphism. In the Oldoinyo Lengai ash, the calcium silicates result from the release of calcium and silicon from wollastonite during the reaction with alkali carbonate. Only in a few spots are the chemical ratios appropriate for growth of the

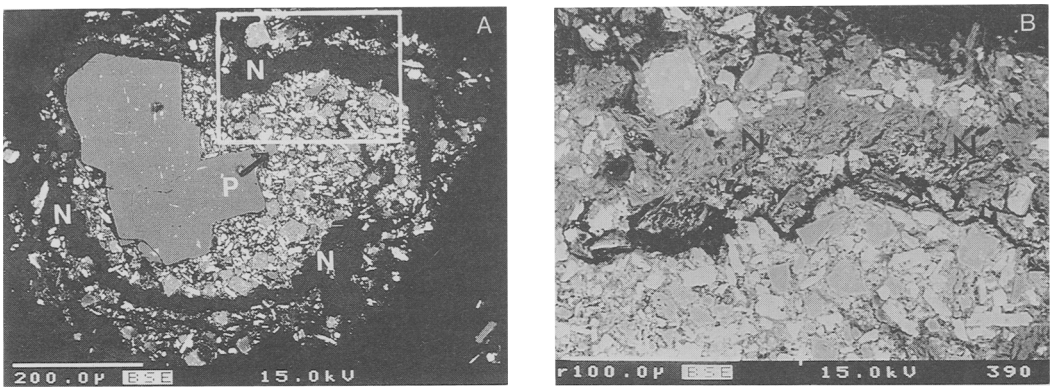

FIG. 8. BSE images of lapillus 8. A shows concentric layes of low reflectance Na_2CO_3 (N). The fine-grained area contains a rounded body of Na,K,Ca-phosphate-carbonate (P). The large grain is nepheline with concentric inclusion of pyroxene and apatite. B is an enlargement of the area outlined in A showing a zone of elongated grains of Na_2CO_3 (N).

Table 6, Na, K, Ca phosphate - "carbonate" *intergrowths*

	1	2	3
P_2O_5	18.53	20.07	24.25
SiO_2	1.86	1.29	1.51
TiO_2	0.07	0	0.05
Al_2O_3	0.07	0.02	0
FeO	0.31	0.33	0.08
MnO	0.14	0.10	0.10
MgO	0.07	0.03	0
CaO	18.23	19.45	21.91
Na_2O	30.02	31.37	26.21
K_2O	6.34	5.03	4.36
SO_3	1.33	0.89	0.98
Cl	0.44	0.11	0.38
Sum	77.41	78.69	79.83
CO_2(calc*)	(25.6)	(25.7)	(21.6)

* CO_2 equivalent to total Na_2O+K_2O, not adjusted for Na, K ≡ SO_3, Cl

1, 2 Analyses of different parts of same rounded grain, in dust, lapillus 8

3 In combeite/melilite reaction rim around wollastonite, lapillus 16

calcium silicates, and most of the calcium and silicon enters combeite.

Titanite. One grain of titanite was found (Table 3). It contains some Fe_2O_3 and Al_2O_3, and is similar to titanite in the Lengai silicate lavas (Donaldson *et al.*, 1987) and plutonic ijolites and nepheline syenites (unpublished).

Alkali carbonates. Alkali carbonate, with low brightness in BSE images, forms the cement in the lapilli. It also forms monomineralic layers between accretionary shells dominated by the silicate microcrystals (Fig. 8A,B). The alkali carbonate occurs as elongated crystals with a sheaf-like texture. Electron microprobe analyses are very difficult and uncertain for alkali carbonate, and the absolute values of the major elements are subject to unquantifiable errors. The presence of carbon was demonstrated by a special electron microprobe analysis using dolomite as a standard, but was not accurately determined. However it seems quite certain that the alkali carbonate in the Lengai ash is close to Na_2CO_3. Only minor amounts of other elements (Ca, S, K, Cl, Fe, Mn, etc.) were found in a reconnaissance analysis (Table 7), and a thorough study was not made. Analyses of a shell around lapillus 14 showed lower Na_2O, but not as low as the value expected for the hydration product nahcolite: this specimen showed higher sulphur.

Although a positive identification by X-ray diffraction was not obtained, it is tentatively assumed that the Lengai carbonate corresponds to the mineral natrite, almost pure Na_2CO_3, from the Khibina and Lovozero alkali massifs (Khomyakov, 1982).

Na,K,Ca phosphate–(carbonate?). Rounded bodies of alkali-calcium phosphate composition occur in both combeite/melilite reaction rims and in the cemented dust clouds (Fig. 8A). Analytical totals (Table 6) are low, but addition of the CO_2 equivalent for the Na_2O and K_2O yields totals close to 100%. Back-scattered electron images are mottled at the sub-micrometre level, suggesting an intergrowth of two or more phases. The bulk analysis can be represented fairly closely by a mixture of alkali carbonate and alkali-bearing apatite with minor amounts of other possible

Table 7 Analyses of alkali carbonates

	1	2	3	4	5	6
P_2O_5	0.04	-	-	0.06	-	-
SiO_2	0.06	-	-	0.12	-	-
TiO_2	0.03	-	-	0	-	-
Al_2O_3	0.01	-	-	0	-	-
FeO	0.15	-	-	0	-	-
MnO	0.14	-	-	0	-	-
MgO	0.01	-	-	0.02	-	-
CaO	0.27	-	-	0.09	-	-
Na_2O	54.00	54.59	58.5	47.23	50.0	35.9
K_2O	0.18	0.02	-	0.24	-	-
SO_3	0.30	-	-	1.51	-	-
Cl	0.15	-	-	0.21	-	-
CO_2	n.a.	41.04	41.5	n.a.	35.5	51.1
H_2O+	n.a.	-	-	n.a.	14.5	13.0
H_2O-	n.a.	3.7	-	n.a.	-	-
Sum	55.34	99.35	100.0	49.48	100.0	100.0

1. Alkali carbonate, zone between two concentric dust layers, lapillus 8.
2. Natrite, Khibina and Lovozero alkali massifs, Kola, U.S.S.R. (Khomyakov, 1982). Spectrographic analyses show traces of Ca, Mn, Fe, Mg, Al, Si, Ti, Cu.
3. Theoretical Na_2CO_3.
4. Alkali carbonate layer on carbonatite fragment, lapillus 14.
5. Theoretical $Na_2CO_3 . H_2O$.
6. Theoretical $NaHCO_3$ (nahcolite).

minerals. Concerning the proposed apatite, unpublished electron microprobe analysis of apatite in Lengai carbonatite lava show approximatley 30 wt.% P_2O_5, 2 SiO_2, 43 CaO, 3 K_2O, 8 Na_2O, 5 F, 0.7 Cl, 11 others. A possible interpretation that could be tested experimentally is that a liquid dominated by alkali phosphate-carbonate crystallized rapidly to give a fine-grained intergrowth of the proposed alkali-rich apatite and carbonate.

Sylvite. Although this mineral was not positively identified, the excellent correlation between the X-ray signals for K and Cl provides a plausible basis for the identification.

Fluorite. See above for the evidence of the presence of this mineral in the carbonate matrix.

Glass inclusions and unknown inclusions. Glass inclusions are common in nepheline and pyroxene grains. They are highly alkaline and some have rather low Al_2O_3. Analytical totals are low (Table 8), implying the omission of one or more light elements in the analysis, possibly CO_2. In most respects, these glass compositions are similar to those of interstitial glasses in Oldoinyo Lengai

Table 8. Analyses of glasses and unidentified material

	1	2	3	4	5	6
P_2O_5	0.07	0.24	0.27	1.01	0.53	0.76
SiO_2	48.69	43.94	44.19	3.29	15.93	34.60
TiO_2	0.71	0.77	1.35	1.56	5.20	2.73
Al_2O_3	10.55	9.85	9.23	1.10	0.81	1.94
Fe_2O_3	9.07	9.24	9.81	2.02	10.76	25.58
MnO	0.18	0.11	0.35	0	0	1.50
MgO	0.04	0	0	0	0	3.48
CaO	2.94	3.09	5.08	3.85	16.81	4.01
Na_2O	10.44	13.88	12.87	33.80	22.74	14.02
K_2O	6.51	6.69	7.19	0.49	0.03	6.82
SO_3	0	0	0	49.42	23.85	9.98
Sum	89.20	87.81	90.34	96.54	96.66	105.42

1. Glass inclusion in nepheline, lapillus 10 (average of 3 points of similar composition)
2,3. Glass inclusions in pyroxene, lapillus 12.
4,5. Inclusions in melanite, lapillus 11.
6. Phase at interface between pyroxene and combeite, lapillus 7 (average of 2 analyses) Total includes 0.38 wt % Cl. (Na_2O variable - 13.50 and 14.55 wt%)

silicate lavas (Donaldson *et al.*, 1987). More unusual materials have been found in two other grains. A garnet contains irregular areas of material that is unusually high in Na_2O and SO_3 (Table 8, analyses 4,5), together with variable amounts of SiO_2, TiO_2 FeO and CaO. Compositionally these materials are intermediate between Ti-andradite and Na_2SO_4, while the low totals again imply the presence of unanalysed light elements, perhaps CO_2. Another unknown material occurs at the interface between pyroxene and combeite (Table 8, analysis 6). It is highly alkaline (Na_2O 14 and K_2O 7 wt.%), iron-rich (FeO 23 wt.%), sulphur-rich (10 wt.% SO_3), and alumina poor (2%).

K,Na,Fe,Mn,Si,P,Cl-sulphide-carbonate. A sulphur-rich phase occurring as rounded to amoeboid inclusions in the combeite-bearing coronas shows a moderately continuous chemical trend from P 0.8, Si 1.8, Fe 32, Mn 1, Ca 1, Na 3, K 10, S 24, Cl 1, element total 74 wt.% to 0.1, 1.0, 33, 1.6, 0.5, 1.6, 15, 32, 1, 86, respectively (Table 9). Semiquantitative electron microprobe analyses for carbon on Au-coated sections demonstrate that it is present in substantial amounts, but the absolute value could not be determined accurately. It seems likely that the carbon is present as the CO_3 component. Additional oxygen coupled with other elements, especially P and Si, is plausible but indeterminate from the present study. There is too much Cl to be assigned to a chlorapatite component, and sylvite is a likely reservoir. Two years after the original study, we decided to make further analyses for Ba, Sr and rare-earth elements. Unfortunately the surfaces had become covered with a fine white powder in spite of storage in a dessicator. Analyses of Ba and Sr on two further low-sulphur inclusions showed 0.7–1.0 wt.% Ba and less than 0.05% Sr.

The concentrations for the individual elements are plotted against the total concentration of analysed elements in Fig. 9. The major constituents (S, Fe + Mn, K + Na) show well-defined trends against the total concentration of the analysed elements with only weak scatter about the dashed lines. The trend for P is well defined, and extrapolates to zero as the S and (Fe + Mn) reach their maximum values. The trend for Si also decreases but not to zero. In contrast, the concentrations of Ca and Cl are rather erratic.

Table 9 EMP analyses of S-rich grains in Lengai ash

wt.% Grain	1-A	1-A'	1-C	1-C'	2-A	2-A'	2-C	2-C'	3-A	3-B	12-E	12-E'	12-F	12-F'
P	.38	.32	.14	.22	.81	.75	.43	.41	.08	.15	.65	.68	.60	.57
Si	1.73	1.78	.82	.78	1.82	1.87	.83	.76	1.18	1.11	2.14	2.30	2.30	2.24
Ti	.03	.05	.04	.05	.02	.00	.11	.09	.01	.02	.06	.08	.02	.01
Al	.01	.00	.05	.05	.03	.04	.02	.00	.03	.35	.03	.00	.01	.03
Fe	34.02	33.00	32.40	33.16	31.94	31.47	38.02	39.75	33.05	35.10	36.85	36.12	33.32	34.00
Mn	1.70	1.58	1.60	1.70	1.22	1.07	.78	1.05	1.54	1.60	1.26	1.22	1.43	1.42
Mg	.07	.03	.03	.00	.00	.04	.18	.17	.00	.00	.00	.00	.05	.07
Ca	1.15	.99	.62	.57	.65	.69	.94	.66	.53	.44	.56	.60	.85	.82
Na	2.69	2.90	3.18	3.18	3.09	3.17	4.28	4.37	1.58	1.46	2.97	3.12	3.45	3.32
K	12.18	11.83	14.02	13.72	10.02	10.22	8.50	8.66	14.97	13.85	9.61	9.04	9.95	9.53
S	26.92	27.45	30.11	30.33	24.32	24.23	26.62	27.20	32.50	29.68	21.51	20.58	22.23	22.92
Cl	1.17	1.19	1.00	1.03	.52	.46	.44	.35	.71	.99	.93	1.02	1.08	1.08
Sum	82.05	81.12	84.01	84.79	74.44	74.01	81.15	83.47	86.18	84.75	76.57	74.76	75.29	75.99
atomic %														
P	.59	.50	.21	.32	1.39	1.30	.69	.64	.11	.22	1.14	1.21	1.03	.97
Si	3.01	3.06	1.38	1.30	3.46	3.58	1.47	1.31	1.94	1.89	4.08	4.48	4.37	4.23
Ti	.03	.05	.04	.05	.03	.00	.11	.09	.01	.02	.07	.09	.02	.01
Al	.01	.00	.09	.08	.07	.07	.04	.00	.05	.62	.05	.00	.01	.07
Fe	29.75	29.01	27.28	27.74	30.64	30.26	33.77	34.46	27.35	29.96	35.33	35.40	31.80	32.19
Mn	1.51	1.41	1.37	1.44	1.19	1.04	.71	.92	1.30	1.39	1.23	1.22	1.39	1.36
Mg	.15	.06	.06	.00	.00	.09	.24	.34	.00	.00	.00	.00	.11	.16
Ca	1.40	1.21	.72	.66	.87	.93	1.17	.80	.61	.53	.74	.82	1.13	1.08
Na	5.72	6.18	6.50	6.47	7.21	7.40	9.23	9.19	3.17	3.02	6.91	7.43	8.00	7.64
K	15.21	14.84	16.86	16.39	13.73	14.03	10.79	10.73	17.69	16.89	13.14	12.65	13.56	12.89
S	41.01	42.03	44.16	44.19	40.63	40.59	41.16	41.05	46.85	44.13	35.90	35.12	36.95	37.79
Cl	1.61	1.65	1.33	1.36	.78	.70	.62	.47	.92	1.33	1.41	1.58	1.63	1.61

Grain numbers refer to host lapillus, letters to individual grains.

The sum of K + Na is nearly constant with about 10% scatter. A BSE image (Fig. 7) of one of the inclusions shows strong variations of brightness at the micrometre scale, and the levels indicate at least two and possibly four different phases. Images of other inclusions did not show such dramatic contrast, and any intergrowths in these inclusions must be below the spatial resolution of the BSE system. The sum total of the evidence is consistent with a chemical trend in a differentiated series of liquids that is now represented by a fine-scale intergrowth of several minerals as yet unidentified. Some small scatter about the main trend would be the consequence of the local availability of elements during the reaction of the carbonate liquid with the silicates during the formation of combeite, melilite, etc.

Fig. 10 contains X-ray scanning images from Si, S, K and Fe in the inclusion shown in Fig. 7. Bearing in mind the problems of poor resolution and absence of matrix corrections, it is apparent that there is a good negative correlation between Si and S, a moderate positive correlation between Fe and S, a poor positive correlation between K and both Fe and S, and a poor negative correlation between K and Si.

The shortfall in the analytical totals can be largely explained by assuming that an Fe sulphide is a dominant phase, and assuming that the other elements may be combined either with each other, or with CO_2 or oxygen to form plausible potential minerals such as apatite (Ca, P and some Cl), calcite (remaining Ca and assumed CO_2) sylvite (K and Cl), and Si, Ti, Fe, Mn and Al oxides. K in excess of that required to match Cl, could be allocated to potential K_2CO_3 though potential KFe-sulphides such as bartonite, $K_3Fe_{10}S_{14}$ (Czamanske *et al.*, 1981; Evans and Clark, 1981), rasvumite, KFe_2S_3 (Sokolova *et al.*, 1970; Czamanske *et al.*, 1979; Clarke and Brown, 1980) and djerfisherite, $K_6Na(Fe,Cu,Ni)_{14}S_{24}Cl$ (Dmitrieva and Ilyushkin 1975; Czamanske *et al.*, 1979) are possibilities.

To conclude this section, it is quite clear that many technical challenges in mineral identification and chemical analysis remain, and that the above data and comments must be regarded as a reconnaissance.

Discussion

The above mineralogy and petrology can be explained by (i) incomplete reaction between an ijolitic magma carrying phenocrysts and some

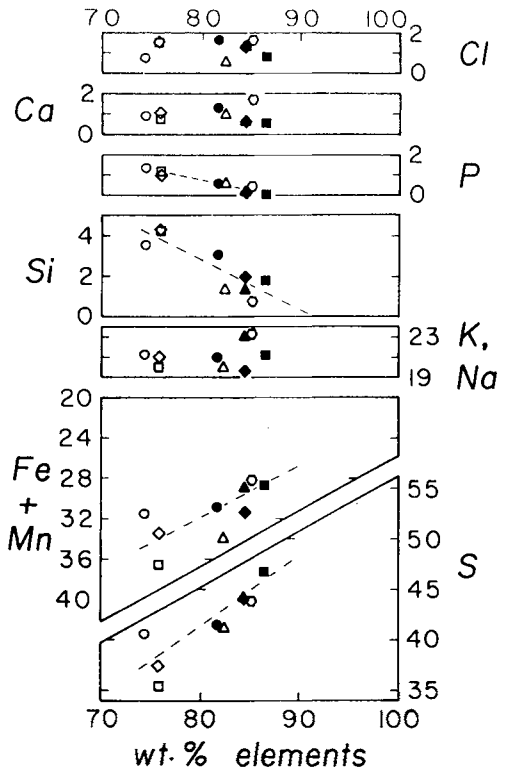

FIG. 9. Trend of element concentrations *vs.* total wt.% of the analysed elements for the S-rich inclusions. The symbols are keyed to the analyses in Table 9. The dashed lines were inserted by eye, and have no statistical significance.

ijolitic rock fragments with a carbonatite magma, and (ii) rapid crystallization of the heterogeneous products. Minor amounts of sulphur- and phosphate-rich components separated out as liquds and crystallized rapidly into fine-grained intergrowths. The mineral assemblages show common features resulting from the general effects of the magma mixing but the details are very complex and vary from one ash lapillus to another. In general, an ash lapillus may contain one or more macrocrysts or rock fragments surrounded by a dust cloud of microphenocrysts, all cemented by alkali carbonate. Some lapilli contain several shells that indicate a complex dynamic history in the ash cloud.

Petrography. The petrography shows that two sets of mineral phases were produced immediately prior to, and during, the 1966 ash eruption. The *first set* definitely contains euhedral crystals of nepheline, Ti-garnet and Ti-magnetite, some of which have inclusions of peralkaline glass. Because the macrocrysts of wollastonite and pyroxene have rounded margins which result from a corrosive reaction with carbonatite magma, it is not possible to use the surface morphology as a guide to the provenance. However, the attachment of a corroded pyroxene macrocryst to euhedral crystals indicates growth as a phenocryst, and delicate oscillatory zoning in another corroded crystal also indicates unhindered growth in a magma. Hence, pyroxene and probably wollastonite join the other three minerals as evidence for the presence of an ijolitic magma just prior to eruption. This is not surprising since ijolite has been a persistent type of magma throughout the history of the volcano (Dawson, 1989).

The *second set* of mineral phases is associated with minor rounded bodies that result from the crystallization of residual liquids. All these materials are the products of interaction of the above starting materials. Particularly dramatic are the reaction coronas around the corroded wollastonite and pyroxene crystals which became unstable in the presence of carbonatite magma. In contrast, the nepheline, garnet and magnetite did not react. The principal product of the corrosion of the wollastonite and pyroxene is combeite. Other products are melilite and two calcium silicates (possibly related to larnite and rankinite).

Also present in the coronas and the dust clouds are two types of rounded and amoeboid bodies of fine-grained intergrown minerals which are attributed to the rapid crystallization of liquids. The first type is dominated by *Na,K,Ca phosphate–carbonate,* whose bulk composition can be matched by a mixture of alkali carbonate and alkali apatite plus minor phases. The second type, which is dominated by *alkali–iron–sulphide–carbonate,* shows a compositional series with S varying from 21 to 32 wt.%. Complex mixtures of alkali carbonate, iron sulphide, and several other minerals are needed to account for the bulk compositions.

Most of the cement is sodium carbonate, which would have crystallized directly from the carbonatite liquid. Because of the rounded amoeboid outlines of the phosphate–carbonate and sulphide–carbonate bodies, these components are assumed to be immiscible with respect to the dominant carbonatite liquid at the time of quenching and crystallization. The carbonate cement is peppered with tiny grains of sylvite and fluorite which probably derived from minor substituents in the carbonatite magma. All of the liquid compositions appear to have contained minor or trace amounts of elements (e.g. P) that

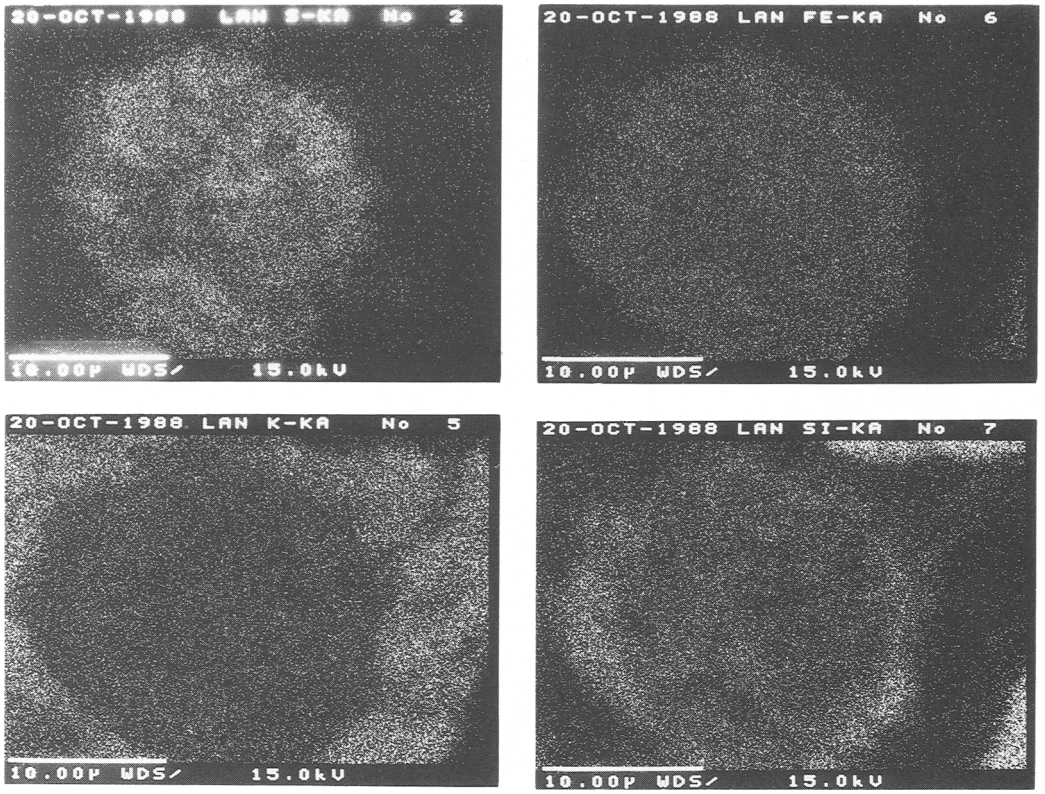

FIG. 10. Scanning images for X-rays from Si (bottom right), S (top left), K (bottom left) and Fe (top right) in the S-rich inclusion shown in Fig. 7.

were concentrated in one of the other liquids, as would be expected for immiscible liquids in equilibrium or reaction relation. It is worth noting that the immiscible liquids in the low-pressure Lengai carbonatites differ quite markedly from those in compound inclusions in mantle-derived megacrysts and pyroxenites (Andersen *et al.*, 1987). The mantle ones are Ni,Co,Cu-bearing FeS-rich liquid coexisting with silicate melt and supercritical CO_2.

Composition of the carbonatite. In our earlier discussion on the interaction of the pyroxene and wollastonite with alkali carbonate to form combeite and melillite (Dawson *et al.*, 1989), we suggested that the carbonatite may have been compositionally similar to that extruded in 1960 (Dawson, 1962*a*). In addition to containing approx. 32 wt.% Na_2O, some of which would be consumed to produce combeite, it also contains 14% CaO, 7% K_2O, 1.5% SrO and SO_3, 3% Cl, 1% P_2O_5 and 0.3% FeO. These components would need to be precipitated prior to the crystallization of the pure Na_2CO_3 phase which cements and overgrows the lapilli. Because these components can be attributed to the various mineral phases and rounded/amoeboid bodies in the coronas and dust cloud, there appears to be no mass balance problem. However some elements, including sulphur, may have escaped prior to the explosive eruption, as witnessed by sulphur precipitation around the fumaroles.

Physical conditions. Assessment of the conditions for the reaction between the silicates and the carbonatite is hampered by the lack of experimental data on compositionally-appropriate systems. Fortunately it can be assumed that the pressure was low in this volcanic setting, and that the temperature and compositional parameters are the ones to be assessed. Moir and Glasser (1974) found that a 1 : 2 : 3 phase, approximating to the Lengai combeite, is stable down to at least 650° and up to 1300 °C in the volatile-free system Na_2SiO_5–$CaSiO_3$. In the system CaO–SiO_2–CO_2 (Shmulovich, 1968), larnite (which forms at a higher temperature than rankinite) was synthesized at temperatures

between 800 °C (25 bar) and 1000 °C (250 bar). There are no pertinent data to constrain the stability limits of the Lengai 'larnite' and 'rankinite' in which MgO, FeO and alkalis are significant components, though a shift to lower temperature might be suggested. A lower limit is the extrusion temperature of alkali carbonatite magma—580 °C at one atmosphere (Dawson *et al.*, 1990). Hence the reactions between silicates and carbonatite might have taken place mainly within a temperature range of about 600 to 800 °C.

The formation of a sulphide-bearing immiscible liquid suggests that the oxygen fugacity was low enough to prevent conversion to sulphates and iron oxides. Further evidence on the redox state arises from the crystallization of Ti-garnet immediately prior to the eruption. Virgo *et al.* (1976) have shown that various Ti-andradites, some from carbonatite volcanoes (Kaiserstuhl, Rusinga), have crystallized at an oxygen fugacity between the Fe-quartz-fayalite and Fe-wüstite buffers.

Decarbonation. The explosive nature of the August 1966 eruption contrasts with the quiet release of combined volatiles in the preceding extrusions of carbonatite lavas, and requires an explanation. Some factor must have forced the evolution of the volatiles as a gas phase. The reaction of the carbonatite with the pyroxene and wollastonite used up sodium and would certainly cause the release of CO_2, which is a dominant volatile species in the gas released from Oldoinyo Lengai (Javoy *et al.*, 1989).

Liquid immiscibility. Liquid immiscibility has been proposed as the cause of the separation of the alkali carbonatite liquid from a carbonated ijolitic or nephelinitic parent (reviewed by Kjaarsgaard and Hamilton, 1989). Immiscibility between alkali carbonate liquid and alkali silicate liquid was demonstrated at 1–15 kbar and at temperature up to 1250 °C. The compositional extent of immiscibility increases with pressure, and has not been found below 1 kbar. Hence a drop of pressure should promote intermingling of silicate and carbonate liquids.

Dynamic model. We conclude with a dynamic model that is based on some kind of mixing of silicate and carbonate magmas. One possible way to get the mixing is to begin with a chamber containing density- and immiscibility-stratified magmas. A zone of alkali carbonate magma overlay an ijolite magma from which nepheline, Ti-garnet, pyroxene and wollastonite were crystallizing. The upper carbonate part of the chamber was gradually evacuated by the 1960–1966 lava extrusions. This resulted eventually in a fall of pressure to below that required to maintain immiscibility (*ca.* 1–2 kbar), and the ijolitic and residual carbonate liquids intermixed. At this stage the released CO_2 caused a violent eruption with emission of a mixture of silicate and carbonate materials which broke up into a cloud of liquid droplets and crystals. Turbulent mixing during the rapid cooling of the cloud produced the wide range of lapilli, some of which ended up with several shells. During the rapid crystallization, alkylation reactions proceeded and CO_2 continued to escape. Some of the carbonate survived as the sodium carbonate. The minor phosphate and sulphide components became concentrated into immiscible liquids, and finally underwent quench crystallization.

Many details of the mineralogy and chemical processes remain for further study. Because of the fine-grained nature of the intergrowths and the volatility of the components, further mineralogical and chemical studies will be very challenging. Finally, a host of synthesis experiments are needed to define the phase relations for the carbonate–phosphate–sulphide–silicate equilibria.

Acknowledgements

Observation of the 1966 eruption and sample collection was made during a visit by JBD to Tanzania financed by the Carnegie Trust for the Universities of Scotland. Field assistance from the Mineral Resources Division of Tanzania and G. C. Clark is gratefully acknowledged. The collaborative research between Chicago and Edinburgh is supported by a travel grant from NATO 86/333. Financial support was derived from NASA NAG 9-47 and instrumental support through NSF EAR-8415791 and NSF EAR-8608299. JVS is supported by the Consortium for Advanced Radiation Studies with start-up funds from the University of Chicago.

References

Agrell, S. O. (1965) Polythermal metamorphism of limestone at Kilchoan, Ardnamurchan. *Mineral. Mag.*, **34**, 1–15.

——and Gay, P. (1961) Kilchoanite, a polymorph of rankinite. *Nature*, **189**, 743.

Andersen, T., Griffin, W. L., and O'Reilly, S. Y. (1987) Primary sulphide melt inclusions in mantle-derived megacrysts and pyroxenites. *Lithos*, **20**, 279–94.

Bishop, F. C., Smith, J. V., and Dawson, J. B. (1978) Na, K, P and Ti in garnet, pyroxene and olivine from peridotite and eclogite xenoliths from African kimberlites. Ibid. **11**, 155–73.

Clark, J. R. and Brown, G. E., Jr. (1980) Crystal structure of rasvumite, KFe_2S_3. *Am. Mineral*, **65**, 477–82.

Czamanske, G. K., Erd, R. C., Sokolova, M. N.,

Dobrovol'skaya, M. G. and Dmitrieva, M. T. (1979) New data on rasvumite and djerfisherite. Ibid. **64**, 776–8.

——Leonard, B. F. and Clark, J. R. (1981) Bartonite, a new potassium iron sulfide mineral. Ibid. **66**, 369–75.

Dawson, J. B. (1962*a*) Sodium carbonate lavas from Oldoinyo Lengai, Tanganyika. *Nature* **195**, 1075–6.

——(1962*b*) The geology of Oldoinyo Lengai. *Bull. Volcanol.* **24**, 349–87.

——(1989) Sodium carbonatite extrusions from Oldoinyo Lengai, Tanzania: implications for carbonatite complex genesis. In *Carbonatites: genesis and evolution.* (Bell, K., ed.). Unwin Hyman, London, 255–77.

——Bowden, P. and Clark, G. C. (1968) Activity of the carbonatite volcano Oldoinyo Lengai, 1966. *Geol. Rundsch.* **57**, 865–79.

——Smith, J. V., and Steele, I. M. (1989) Combeite ($Na_{2.33}Ca_{1.74}$ others$_{0.12}$)Si_3O_9 from Oldoinyo Lengai, Tanzania. *J. Geol.* **97**, 365–72.

——Pinkerton, H., Norton, G. E., and Pyle, D. M. (1990) Physicochemical properties of alkali carbonate lavas: data from the 1988 eruption of Oldoinyo Lengai, Tanzania. *Geology*, **18**, 260–3.

Dmitrieva, M. T., and Ilyushkin, V. V. (1975) Crystal structure of djerfisherite. *Soviet Physics—Doklady*, **20**, 469–70.

Donaldson, C. H., Dawson, J. B., Kanaris-Sotiriou, R., Batchelor, R. A., and Walsh, J. N. (1987) The silicate lavas of Oldoinyo Lengai, Tanzania. *Neues. Jahrb. Mineral. Abh.* **156**, 247–79.

Evans, H. T., Jr. and Clark, J. R. (1981) The crystal structure of bartonite, a potassium iron sulfide, and its relationship to pentlandite and djerfisherite. *Am. Mineral.*, **66**, 376–84.

Henmi, K., Kusachi, I., and Henmi, C. (1975) Rankinite and kilchoanite from Fuka, the Town of Bitchu, Okayama Prefecture, Japan. *J. Mineral. Soc. Japan*, **12**, 205–14. (Japanese).

Javoy, M., Pineau, F., Staudacher, T., Cheminee, J. L., and Krafft, M. (1989) Mantle volatiles sampled from a continental rift: the 1988 eruption of Oldoinyo Lengai, Tanzania. *Terra Abstracts*, **1**, 324.

Keller, J. and Krafft, M. (1990) Effusive natrocarbonatite activity of Oldoinyo Lengai, June 1988. *Bull. Volcanol.*, **52**, 629–45.

Khomyakov, A. P. (1982) Natrite, Na_2CO_3, a new mineral. *Zap. Vses. Mineral. Obsh.*, **111**, 220–25. (Russian).

Kjaarsgaard, B. A. and Hamilton, D. A. (1989) The genesis of carbonatites by immiscibility. In *Carbonatites: genesis and evolution.* (Bell, K., ed.). Unwin Hyman, London, 308–404.

Kusachi, I., Henmi, C., Kawahara, A. and Henmi, K. (1975) The structure of rankinite. *Mineral. J.*, **8**, 38–47. (Japanese).

Mitsuda, T. and Fukuo, K. (1969) Synthesis of kilchoanite. Ibid. **6**, 17–35. (Japanese).

Moir, G. K. and Glasser, F. P. (1974) Phase equilibria in the system Na_2SiO_5–$CaSiO_3$. *Phys. Chem. Glasses*, **15**, 6–11.

Peterson, T. D. (1990) Petrology and genesis of natrocarbonatite. *Contrib. Mineral. Petrol.*, **105**, 143–55.

Saalfeld, H. (1975) X-ray investigation of single crystals of β-Ca_2SiO_4 (larnite) at high temperatures. *Amer. Mineral.*, **60**, 824–7.

Sabine, P. A. (1975) Metamorphic processes at high temperature and low pressures, and the petrogenesis of metasomatized and assimilated rocks of Carneal, Co. Antrim. *Phil. Trans. Roy. Soc. A*, **280**, 225–67.

Suburi, S., Kusachi, I., Henmi, C., Kawahara, A., Henmi, K., and Kawada, I. (1976) Refinement of the structure of rankinite. *Mineral. J.* **8**, 240–6. (Japanese).

Sarkar, S. L. and Jeffrey, J. W. (1978) Electron microprobe analysis of Scawt Hill bredigite-larnite rock. *J. Amer. Ceram. Soc.*, **61**, 177–8.

Shmulovich, K. I. (1968) Stability of larnite in the CaO–SiO_2–CO_2 system. *Dokl. Acad. Sci. USSR, Earth Sci. Sect.*, **177**, 142–5.

Smith, D. K., Majumdar, A. J. and Ordway, F. (1961) Re-examination of the polymorphism of dicalcium silicate. *J. Amer. Ceram. Soc.*, **44**, 405–11.

Smith, J. V., Steele, I. M. and Dawson, J. B. (1988) Carbonate ash from Oldoinyo Lengai, Tanzania: combeite, larnite, rankinite: K,Na,Fe,Mn,Si,P,Cl–sulfide and carbonate differentiates; sodium carbonate; Na,Ca,K–phosphate; reaction textures. *Geol. Soc. Amer. Abstr.*, with Program **20**, A103.

Sokolova, M. N., Dobrovol'skaya, M. G., Organova, N. I., Kazakova, M. E., and Dmitrik, A. L. (1970) A sulfide of iron and potassium—the new mineral, rasvumite. *Zap. Vses. Mineralog. Obshch.*, **99**, 712–20.

Taylor, H. F. W. (1971) The crystal structure of kilchoanite $Ca_6(SiO_4)(Si_3O_{10})$, with some comments on related phases. *Mineral. Mag.*, **38**, 26–31.

Virgo, D., Huggins, F. E., and Rosenhauer, M. (1976) Petrologic implications of intrinsic oxygen fugacity measurements on titanium-containing silicate garnets. *Carnegie Institution of Washington Yearbook*, **75**, 730–5.

Zharikov, V. A. and Shmulovich, K. I. (1969) Experimental study on the system CaO–SiO_2–CO_2 between 800–1000° and at pCO_2 = 50–500kg/cm^3. *Dok. Acad. Sci. USSR, Earth Sci. Sect.*, **188**, 170–3.

[*Manuscript received 17 June 1991: revised 20 July 1991*]